Micro-Robot Leg Design for SMART DUST using Improved Inchworm Motor

Y. H. Chee, C. Tsang
Department of Electrical Engineering and Computer Sciences
Cory Hall
University of California at Berkeley
Berkeley, CA 94720

ABSTRACT

This paper discusses the design of micro-robot legs based on the skiing principle using an improved version of the inchworm motors for the SMART DUST program. Four inchworm motors are attached to each of the two parallel sides of a SMART DUST mote to serve as the ski legs and support legs for the dust mote. The ski legs push the micro-robot at 75° from the surface and are capable of moving a micro-robot with maximum mass of 12.3mg by 40μm per ski cycle. Each inchworm motor measures 1000μm x 250μm x 150μm and has a minimum force density (at max shuttle displacement) of 129μN/mm^2 at 33V. This translates to a payload of 130 times its own weight. The force density at zero shuttle displacement is 206μN/mm^2. The average work done per inchworm cycle is 3.66nJ with an efficiency of 36%. The maximum shuttle displacement is 96μm. The micro robot legs are designed based on the 2-poly SOI process (Iolanthe Process) available at UC Berkeley.

INTRODUCTION

The rapid development of MEMS micro-robots in the recent years offers many new and exciting applications. Examples include micro-inspectors and micro-assembly tools industrial applications, micro-unmanned surveillance vehicles and micro-weapons for military applications, and micro-surgeons for medical applications.

Several methods of motion and actuation for MEMS micro-robots have been proposed. Suzuki et al. proposed the concept of creating insect-like micro-robots made from surface micromachined polysilicon plates and polyimide joints [1]. Ataka et al. designed polyimide bimorph actuators for a ciliary motion system [2]. Kladitis et al. fabricated some micro-robots based on thermal expansion of silicon [3]. Unfortunately, these micro-robots suffer from the pitfalls of either complicated fabrication process or high operation voltage that are not compatible with conventional electronics and most importantly, low energy efficiency and low payload. To address these issues, Yeh et al. have proposed using electrostatic stepper actuators for actuation, micromachined hinges for joints and folded silicon plates for legs [4]. In 1999, Yeh et al. demonstrated an inchworm motor fabricated in a single mask Silicon-on-Insulator (SOI) process that is able to achieved a force density of 87uN/mm^2 at 33V and energy efficiency of about 8% [5].

This paper presents the design and expected results of a micro-robot for the SMART DUST program at UC Berkeley [6]. We proposed a new method of motion based on the skiing principle and described an improved inchworm motor design to achieve a high force density and high payload. The micro-robot legs can be implemented on a two poly-silicon SOI process [7].

FABRICATION PROCESS

The micro-robot legs will be fabricated in the Iolanthe Process available at UC Berkeley [7]. The process uses a SOI wafer with 40μm single crystal silicon layer, 2μm buried oxide layer and 150μm substrate layer. The silicon layer is patterned using Deep Reactive Ion Etching (DRIE) with a maximum aspect ratio of 13. Glass is then deposited, re-flowed and planarized to fill out the DRIE etch holes. Two structural layers (Poly1, Poly2) are then deposited, followed by a backside etch. Finally, the oxide is released. The finished cross-section of this process is shown in Fig. 1.

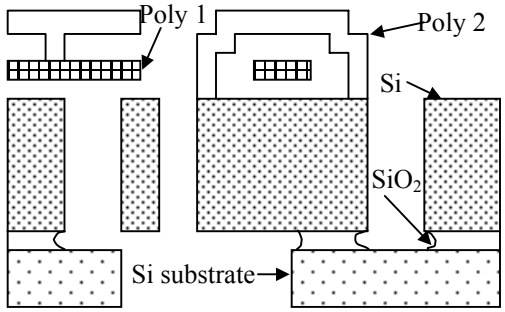

Fig 1: Finished cross-section of the Iolanthe Process.

METHOD OF MOTION

The method of motion of our proposed design is based on the skiing principle. Each dust mote has a volume of 1mm^3 and a mass of 5mg. We attached two sets of robot legs to two sides of the SMART DUST mote as shown in Fig 2.

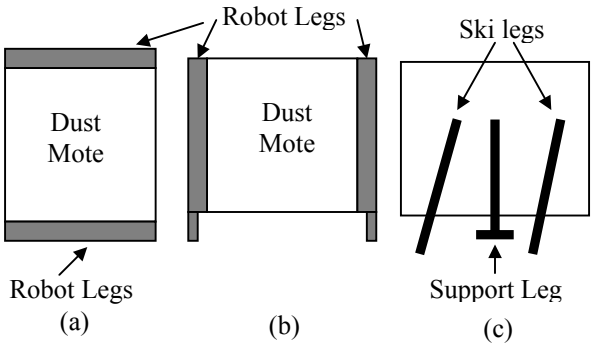

Fig 2. SMART DUST mote with two sets of robot legs attached. (a) top view (b) front view (c) side view showing one set of micro-robot leg.

The operation of the robot legs is described in Fig. 3. Initially, the support leg is off the surface and the ski legs supports the entire weight of the dust mote. Then, the ski legs are linearly displaced at an angle θ to the horizontal. This stroke results in a vertical and horizontal displacement of the body. The support leg is then lowered to support the weight of the body and this allows the ski legs to return to their original positions. Finally, the support leg lowers the body to its initial height, allowing the ski legs to repeat the cycle.

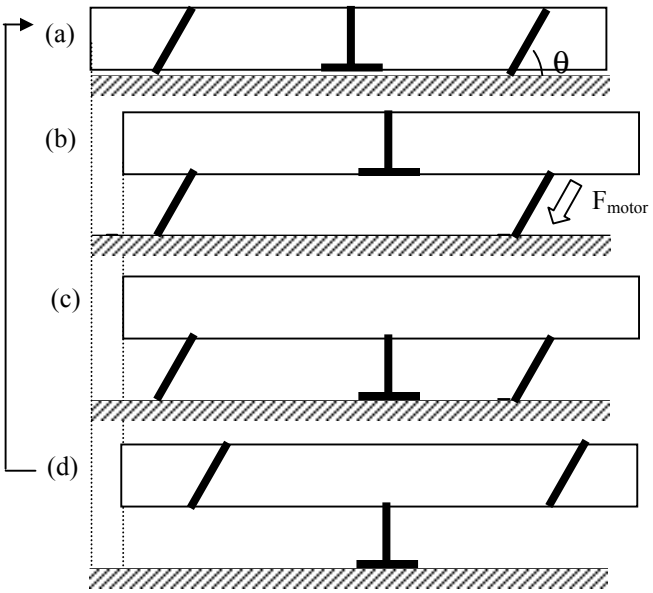

Fig. 3. (a) Initial position of ski legs and support leg. (b) Ski legs move body forward and upward. (c) Support leg lowers to support body (d) Ski legs restore to original position. Support leg moves back to original position and cycle repeats.

The ski legs' force needs to be large enough to overcome the weight of the robot. A small angle will result in large horizontal displacement but may cause the legs to slip if the horizontal force is greater than the frictional force. Thus, ski leg's force and the angle need to satisfy the following conditions.

$$F_{motor} \sin\theta \geq mg \quad (1)$$

$$F_{motor} \cos\theta \leq \mu(mg + F_{motor} \sin\theta) \quad (2)$$

IMPROVED INCHWORM MOTOR

Principle of Operation

The inchworm motor essentially consists of a shuttle (which acts as the robot's leg) and two x-y actuators as shown in Fig 4. Each x-y actuator has a pawl that engages and drives the shuttle in a repeated sequence as shown in Fig 5. Two springs in the x and y direction provide the force to restore the actuator to its original position. Thus large displacement and large force motion can be achieved by accumulating the displacement moved in each inchworm cycle. To improve the engagement between the pawl and the shuttle, teeth are fabricated along their sides.

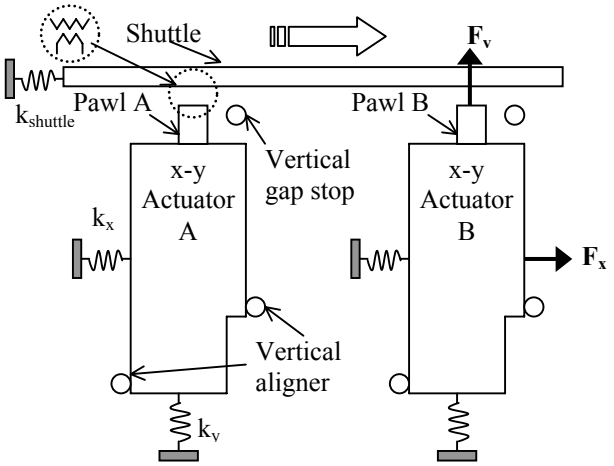

Fig 4. Diagram of an inchworm motor.

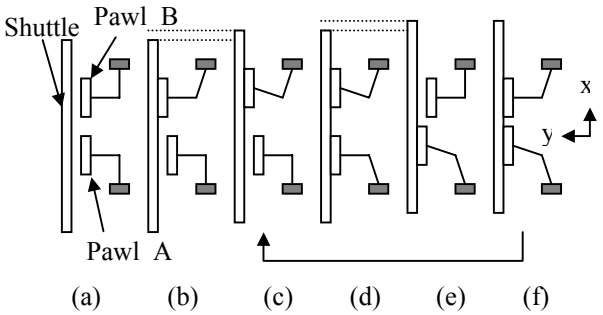

Fig 5. Inchworm motor cycle. (a) Pawls at initial position (b) Pawl B engages shuttle (c) Pawl B drives shuttle (d) Pawl A engages shuttle (e) Pawl B disengages from shuttle as pawl A drives shuttle (f) Pawl B engages shuttle. Repeat from (c).

To maximize the travel distance per inchworm cycle, the pawl should not have any displacement in the x-direction until it engages the shuttles. Yeh et al [5] achieved this using two orthogonal gap closing actuator arrays in each x-y actuator. In this paper, we achieved both x and y actuation with a single array of electrostatic actuators by utilizing electrostatic forces in both the x and y direction.

This approximately reduces the area by half and increases the force density significantly. Decoupling of the x-y motion is achieved by: (1) placing vertical aligners to restrict movement in the x-direction until the pawl engages the shuttle, (2) using vertical gap stop to restrict movement in y-direction after the pawl engages the shuttle.

X-Y Actuator Design

The electrostatic actuator (Fig. 6) consists of two parallel beams with overlap length *l*, thickness *t*, separated by gap g_1. One of the beams is anchored to the substrate and the other is supported by two orthogonal springs in the x-y direction. When a voltage is applied between the two beams, the electrostatic forces in the x and y direction moves the supported beam in the x and y direction respectively. To prevent shorting the two beams, vertical and horizontal gap stops are biased at the same potential as the supported beam. The gap between the supported beam and the horizontal gap stop g_3 determines the step size of the motor. To generate a larger force, an array of the electrostatic actuators is used.

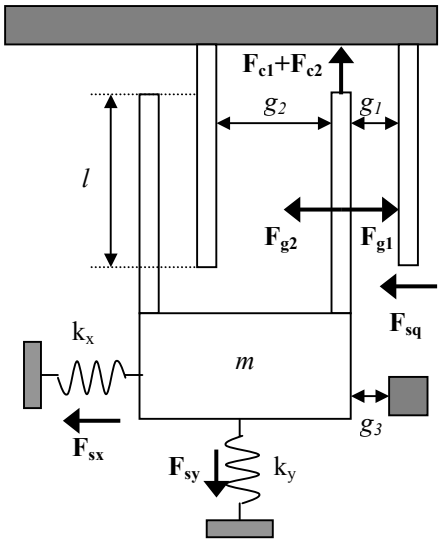

Fig 6. Diagram of two electrostatic actuators

Motion in x-direction

The motion in the x-direction is can be determined by considering resultant force F_x in the x-direction.

$$F_x = F_{g1} - F_{g2} - F_{sx} - F_{sq} - F_L = m\frac{d^2x}{dt^2} \qquad (3)$$

where F_{g1} and F_{g2} are the gap closing electrostatic forces, F_{sx} is the spring restoring force in the x-direction, F_{sq} is the squeeze film damping force, F_L is the load and m is the total mass of the movable beams and its support. The gap closing electrostatic force F_{g1} and F_{g2} is given as

$$F_{g1} = \frac{1}{2}\varepsilon NV^2\frac{tl}{(g_1 - x)^2},\ F_{g2} = \frac{1}{2}\varepsilon NV^2\frac{tl}{(g_2 + x)^2} \qquad (4)$$

where ε is the permittivity of air, N is the number of electrostatic actuators in the array and V is the applied voltage between the anchored and movable beams. Considering the active area of the gap closer, the maximum force density occurs when $g_2 \approx 2.35g_1$. The restoring force from the spring $F_{sx} = k_x x$, where k_x is the spring constant. The squeeze film damping force is significant when the gap between the beams is small compare to the thickness and overlap length of the beams.

For $t < l$, F_{sq} is given by

$$F_{sq} = \frac{N\left(1 - 0.6\frac{t}{l}\right)t^3 l\upsilon}{(g_1 - x)^3}\frac{dx}{dt} \qquad (5)$$

where υ is the viscosity of air. The pull-in voltage V_{PI}, which is the minimum voltage required to close the gap with no external load, is given as

$$V_{PI} = \sqrt{\frac{8}{27}\frac{k_x g_1^3}{\varepsilon t^3 lN}} \qquad (6)$$

Gap g_3 is usually maximized to obtain the largest possible gap size. Hence, to ensure that the gap closer is able to close the gap g3, V_{PI} is designed to be much lower than the applied voltage.

Motion in y-direction

Similarly, the motion in the y-direction can be determined by considering all the forces in the y-direction.

$$F_y = F_{c1} + F_{c2} - F_{sy} - F_r = m\frac{d^2y}{dt^2} \qquad (7)$$

where F_{c1} and F_{c2} are the electrostatic forces in the y-direction, $F_{sy} = k_y y$ (k_y is the spring constant) is the spring restoring force in the y-direction, and F_r is the total frictional force at the vertical aligners. The electrostatic force F_{c1} and F_{c2} is given as

$$F_{c1} = \frac{1}{2}\varepsilon NV^2\frac{t}{(g_1 - x)},\ F_{c2} = \frac{1}{2}\varepsilon NV^2\frac{t}{(g_2 + x)} \qquad (8)$$

Speed

The maximum speed of the inchworm motor is limited by the time the pawl takes to engage (pull-in) and disengage (pull-out) the shuttle. The pull-in time and pullout time is proportional to $1/V^2$ and $\sqrt{1/k}$ respectively. Thus, the speed can be increased by increasing the applied voltage or spring constant.

Work Done and Efficiency

During each inchworm cycle, the pawl first moves in the y-direction and engages the shuttle, and then drives the

shuttle in the x-direction. Thus, the total energy consumed by the inchworm motor per shuttle cycle is the sum of the energy input that contributes to the and x and y-direction motion.

$$E_{input} = N_{step}(\Delta C_{y,gap}+\Delta C_{y,overlap}+\Delta C_{x,gap}+\Delta C_{parasitics})V^2 \quad (9)$$

where $\Delta C_{y,gap}$ is the capacitance change due to the gap-closing effect in the y-direction, $\Delta C_{y,overlap}$ is the capacitance change due to the change in the overlapping length of the electrostatic actuator, $\Delta C_{x,gap}$ is the capacitance change due to the gap-closing effect in the x-direction, $\Delta C_{parasitics}$ is the capacitance change in the parasitic and N_{step} is the total number of steps per shuttle cycle . These capacitance-changes are:

$$\Delta C_{y,gap} = N\left(\frac{\varepsilon t a}{y_2} - \frac{\varepsilon t a}{y_1}\right) \quad (10)$$

$$\Delta C_{y,overlap} = N\left(\frac{\varepsilon t(l+y_0)}{g_1} + \frac{\varepsilon t(l+y_0)}{g_2}\right) - N\left(\frac{\varepsilon t l}{g_1} + \frac{\varepsilon t l}{g_2}\right) \quad (11)$$

$$\Delta C_{x,gap} = N\left(\frac{\varepsilon t(l+y_0)}{g_1-g_3} + \frac{\varepsilon t(l+y_0)}{g_2+g_3}\right) - N\left(\frac{\varepsilon t(l+y_0)}{g_1} + \frac{\varepsilon t(l+y_0)}{g_2}\right) \quad (12)$$

where a is the width of the movable finger, y_1 and y_2 is the initial and final distance between the movable finger and the anchor respectively, $y_0=y_2-y_1$ is the displacement of the finger in the y-direction. The power consumed by the motor is $E_{input}f$, where f is the frequency of operation.

The work done against the restoring force of the springs and for motion in the y-direction does not contribute to any useful work. Hence, the efficiency can be increased by decreasing the spring constants, y-direction force and y-direction displacement. The first two factors trades off efficiency and speed while the third factor is limited by the layout rules.

The total energy supplied for the motion in the x-direction is $N_{step}\Delta C_{x,gap}V^2$. However, only half of this energy is used to move the shuttle and the rest is dissipated. The total energy stored in the restoring spring for the shuttle is $\frac{1}{2}k_{shuttle}\left(g_3 N_{step}\right)^2$ where g_3 is the step size. Hence the work done per shuttle cycle is:

$$WD = \frac{1}{2}N_{step}\Delta C_{x,gap}V^2 - \frac{1}{2}k_{shuttle}\left(g_3 N_{step}\right)^2 \quad (13)$$

The efficiency of the motor is given as $\eta = WD/E_{input}$.

TEST STRUCURES

The most important component of the leg design is the inchworm motor. The main parameters of the inchworm motor are k_x, k_y, $k_{shuttle}$, l and N and they determined the force, operating speed and travel distance of the inchworm motor. To evaluate their effect on performance and test the assumptions used in our calculations, we designed the several inchworm motors with different parameter values as given in Table 1. By varying one parameter of interest at a time from its calculated value, its impact on performance can be determined.

Table 1: Test structures

Test structure	k_x (N/m)	k_y (N/m)	$k_{shuttle}$ (N/m)	l (μm)	N
TS1	3.22	3.5	0.2	100	40
TS2	25.76	3.5	0.2	100	40
TS3	0.403	3.5	0.2	100	40
TS4	3.22	28	0.2	100	40
TS5	3.22	1.75	0.2	100	40
TS6	3.22	3.5	1.6	100	40
TS7	3.22	3.5	0.025	100	40
TS8	3.22	3.5	0.2	150	40
TS9	3.22	3.5	0.2	200	40
TS10	3.22	3.5	0.2	100	80
TS11	3.22	3.5	0.2	100	120

*TS1 is based on the calculated values

The main parameter of the robot leg is its angle of inclination with respect to the horizontal θ as it determined the travel distance and condition when the robot leg slips. Several robot legs with θ = 65°, 70°, 75°, 80° and 85° were designed.

EXPECTED RESULTS AND DISCUSSION

Force Density

A SMART DUST mote is approximately a cubic millimeter in size and weighs 5mg. To move the dust mote, one set of robot legs is attached to the two parallel sides of the SMART DUST mote (Fig 2). Hence, the maximum area for each set of robot legs is approximately 1mm x 1mm. This means that each inchworm motor is approximately 1mm x 0.25mm and has to support a weight of 1.25mg at all times (or a force density of 50μN/mm^2).

From the analysis, the force in the y-direction is proportional to N and independent of l but the force in the x-direction is both proportional to N and l. A minimum force in the y-direction is required to overcome the frictional forces at the vertical aligners. Also, a large force in the y-direction will reduce pull-in time but at the expense of the overhead area. For this design, each x-y actuator array in the inchworm motor consists of two rows of 20 fingers each (i.e. N=40) and l=100μm. To optimize the force density, minimum layout line and space rules are

used. With a gap stop distance of 0.5μm, g_1 = 3.5μm, g_2=8.2μm, g_3=3μm y_0=4.5μm, y_1=5μm and y_2=0.5μm.

The restoring springs are implemented using cantilever beams. To limit the angle of deflection for linear motion, the vertical displacement of the cantilever beams is designed to be at most 10% of its length. As the spring force opposes the electrostatic force, it is important to have a small the spring constant. However, a small spring force will result in a long pullout time and limit the speed of the motor. For this design we have chosen k_x = 3.22 N/m and k_y = 3.5 N/m. To achieved a targeted travel distance of 96μm for the inchworm motor, two springs of length 480μm are connected in series, resulting in $k_{shuttle}$ = 0.20 N/m. With these values, the force density at zero shuttle displacement is 206μN/mm^2 and the minimum force density (occurs at max shuttle displacement) is 129μN/mm^2 Thus, the inchworm motor can lift approximately 130 times its own weight (the volume of the SOI layer is estimated to be etched away by half).

Work Done and Efficiency

The energy input and work done per shuttle cycle without parasitic is 90nJ and 42nJ respectively. Assuming the parasitic contributes an additional 30% to the energy input, an efficiency of 36% is obtained. Hence, the energy input and average work done per inchworm cycle is 3.66nJ and 1.3nJ respectively.

Micro-robot Displacement

The four 4 ski legs are capable of moving a micro-robot with maximum mass of 12.3mg (about 2.5 times the weight of a dust mote) by a horizontal displacement of 40μm per ski cycle. Minimum force of each ski legs is 32μN. With a shuttle displacement of 96μm and from the conditions in (1) and (2), the ski leg is designed to be 75° from the horizontal.

CONCLUSION

This paper has presented the design of micro-robot legs capable of moving at mass of 12.3mg by 40μm per ski cycle using the skiing principle. The legs are driven by improved inchworm motors, which have a minimum force density of 129μN/mm^2 at 33V and operates at an efficiency of 36%.

The inchworm motors can be further optimized for speed by balancing the pull-in time, pull-out time and drive time of each inchworm cycle. This can be achieved by adjusting the spring constants and forces in x and y direction. The limitation of this ski mechanism is that the ski angle θ must be at a relatively large to prevent slipping. Thus, the shuttle displacement of the inchworm motor is translated to the displacement of the robot a factor of cosθ. In addition, this scheme requires the lifting and lowering of the support legs, which does not contribute to any horizontal displacement. Hence efficiency and speed of the robot are reduced. Therefore, there is still plenty of room for improvement and future research in micro-robot legs design based on the skiing principle.

ACKNOWLEDGEMENTS

We would like to thank Prof. K. S. J. Pister for his advice and guidance.

REFERENCES

[1] K. Suzuki, I. Shimoyama and H. Miura, “Insect-model based microrobot with elastic hinges,” IEEE Journal of Microelectromechanical Systems, vol. 3, no. 1, pp. 4-8, Mar. 1994.

[2] M. Ataka, A. Omodaka, N. Takeshima and H. Fujita, “Fabrication and operation of polyimide bimorph actuators for a ciliary motion system,” IEEE Journal of Microelectromechanical Systems, vol. 2, no. 4, pp. 146-150, Dec. 1993.

[3] P. E. Kladitis, V.M. Bright, K. F. Harsh and Y. C. Lee, “Prototype microrobots for micro positioning in a manufacturing process and micro unmanned vehicles,” Proc. of IEEE MEMS ’99, pp. 570-575, 1999.

[4] R. Yeh, E. J. J. Kruglick, K. S. J. Pister, “Surface micromachined components for articulated microrobots,” Journal of Microelectromechanical systems, vol. 5. no. 1, pp. 10-16, Mar. 1996.

[5] R. Yeh, S. Hollar, K. S. J. Pister, “Single mask, large force and large displacement electrostatic linear inchworm motors,” Proc. of the 14th Annual International Conference on Microelectromechanical Systems (MEMS 2001), pp. 260-264, Jan. 2001.

[6] J. M. Kahn, R. H. Katz and K. S. J. Pister, "Mobile Networking for Smart Dust", ACM/IEEE Intl. Conf. on Mobile Computing and Networking (MobiCom 99), Aug. 1999.

[7] http://www-bsac.EECS.Berkeley.EDU/~shollar/iolanthe/iolanthehtml.htm